Sandwich structures with tunable damping properties: on the use of shape memory polymer as viscoelastic core

Pauline Butaud, Emmanuel Foltete, Morvan Ouisse

Sandwich structures with tunable damping properties: on the use of shape memory polymer as viscoelastic core.

Pauline Butaud, Emmanuel Foltête, Morvan Ouisse*

University of Bourgogne Franche-Comt - FEMTO-ST Department of Applied Mechanics, 24 rue de l'pitaphe - 25000 Besanon

Abstract

A Shape Memory Polymer (SMP), the tBA/PEGDMA, is used as viscoelastic core in sandwich structures. The dynamic mechanical characterization of this SMP highlights promising damping properties. The composite sandwich is developed by coupling the SMP with aluminum skins. The SMP core temperature is tuned from the Time-Temperature Superposition Principle through a rainbow calibration curve in order to correspond to optimal values of damping ratio in the frequency range of interest. The damping performances predicted by a Finite Element model are validated experimentally using modal analysis. The experimental results are found to be in good agreement with the predictions of the Finite Element model. Furthermore, it is found that the controlled heating of the SMP core allows damping the structure over a wide frequency range. The methodology which is proposed in this paper is applicable to any viscoelastic material exhibiting frequency - and temperature - dependent high damping properties.

*morvan.ouisse@femto-st.fr

Keywords: damping control, Shape Memory Polymer, adaptive structures

1. Introduction

Shape Memory Polymers (SMPs) belong to the class of smart materials. These materials have found growing interest throughout the last decades. They can be used in a large variety of applications, e.g. actuators, electromechanical systems, clothing manufacturing, morphing and deployable space applications, control of structures, self-healing, biomedical devices and so on [1, 2, 3, 4]. The SMPs have the ability of changing their shape in response to an external stimulus, most typically thermal activation. When the SMP is heated above the glass transition temperature T_g, it is soft and rubbery and it is easy to change its shape. If the SMP is subsequently cooled below T_g, it retains the given shape (shape fixing characteristic). When heated again above T_g, the material autonomously returns to its original permanent shape [5]. Today, SMPs are more and more used for quasi-static and dynamic applications, under various temperature ranges [6], hence deep investigations of the material's properties over wide frequency bands and temperature ranges are required.

Indeed, it turns out that efficient Shape Memory effects are associated to fast transitions between stable glassy and rubbery states with large elasticity gap, inducing high loss factor values at glass transition [7, 8]. In SMP-related open literature, various experimental results provide loss factors values at glass transition. The typical values which are reported vary between 0.5 [9] and more than 2.5 [10], most of them being between 1 and 2 [11, 12, 13, 14]. To the authors' knowledge, this intrinsic property remains unexploited.In this

paper we investigate the use of SMP for the design of composite structures for damping applications.

The use of composite materials in aeronautics, aerospace or automotive is increasingly considered as they often exhibit a higher stiffness with low density compared to conventional materials. Nevertheless they usually have a poor dynamic behavior because of their high rigidity and low damping properties. The control and the reduction of the noise and vibration are then at the center of current issues. Vibration and noise in dynamic systems can be reduced by a number of means. Active control, using for example piezoelectric materials, has many advantages such as adaptivity, high precision and performance controllable systems [15]. However active controllers are very sensitive to variations and uncertainties of system parameters [16] even if distributed strategies can enhance performances while increasing robustness [17, 18]. On the other hand, passive damping treatments lead to reliable, low cost and robust vibration control [19, 20]. A lot of research has so focused on composite structures embedding viscoelastic materials to damp vibrations [21, 22, 23]. In particular, many people have studied the design optimization of multilayers structures [24, 25, 26] by varying the thickness of the viscoelastic layer, the fiber orientation or the aspect ratio of the structure.

In this work, we want to demonstrate that the tuning of the damping properties of the structure can be achieved through the control of the temperature of the viscoelastic core. A sandwich structure composed of aluminum skins and SMP core is designed and the ability of the SMP to reach very high loss factor values at glass transition is used to control the wave propagation. Time-Temperature Superposition [27] is commonly used to reduce the

characterization time, based on the principle that an equivalence occurs between (growing) frequency and (decreasing) temperature, which appears to be valid for a large set of polymers. In particular, the damping capacities of a given material can be characterized through the analysis of the loss factor on a reduced set of temperatures and frequencies using Dynamical Mechanical Analysis (DMA). The highest values of loss factor being obtained at the glass transition, SMPs may potentially be materials of first interest [28]. Among the various possibilities, the SMP core temperature is tuned from the Time-Temperature Superposition Principle to correspond to optimal values of damping ratio in the frequency range of interest. The controlled heating of the SMP core allows to damp the structure on a wide frequency range. The damping capabilities are illustrated through numerical simulations and are validated by experimental tests.

The organization of this paper is as follows. The Shape Memory Polymer and its properties are described in Section 2. Section 3 shows the tuning strategy of the SMP damping properties by the temperature. The Finite Element model of the SMP composite structure is presented in Section 4. The validation of the methodology through experimental tests is discussed in Section 5. Section 6 gives some final conclusions and remarks.

2. SMP material and mechanical properties

2.1. SMP elaboration

The tBA/PEGDMA, studied by Srivastava et al. [29] is chosen for this study. It is elaborated at the FEMTO-ST Department of Applied Mechan-

ics following the procedure described in Yakacki et al. [30]. The Shape Memory Polymer has been synthesized by manually mixing 95 wt% of the monomer tert-Butyl Acrylate (tBA), with 5 wt% of the cross-linking agent poly(ethylene glycol) dimethacrylate (PEGDMA) (with typical molecular weight $M_n = 550$ g/mol). The photoinitiator, 2,2-dimethoxy-2-phenylacetophenone (DMPA), is added to the solution at a concentration of 0.5 wt% of the total weight. The liquid mixture is then injected between two glass slides separated by a 2.2 mm spacer. The polymerization is initiated by exposing the solution to UV light during 10 minutes and achieved by heating the polymer at 90°C for 1 hour. The plates produced are machined whenever necessary. The elaborated material has an apparent Young's modulus of 2200 MPa (±15%) and a Poisson's ratio around 0.37, in quasi-static state at 22°C. The glass transition temperature of this SMP in quasi-static state is between 45°C and 55°C [31].

2.2. SMP dynamic characterization

A Dynamic Mechanical Analysis (DMA) of the SMP has been performed using a METRAVIB DMA50 [31]. The master curves obtained by the Time-Temperature Superposition Principle (TTSP) are given in Figure 1 where the temperature evolution of the shift factor a_T is expressed according to Williams- Landel-Ferry (WLF) law [32] by

$$\log(a_T(T)) = \frac{-C_1^0(T - T_0)}{C_2^0 + (T - T_0)} \ , \tag{1}$$

with $C_1^0 = 10.87$ and $C_2^0 = 32.57$ K for a reference temperature T_0 of 40°C. This expression has been established and validated on the temperature range

tested by DMA between $T = 30°C$ and $T = 90°C$.

The frequency dependence of the viscoelastic material's properties is supposed to be described by a complex modulus $E^*(\omega, T)$:

$$E^*(\omega, T) = E'(\omega, T)(1 + j\tan(\delta)) \ , \tag{2}$$

where $\omega = 2\pi f$ is the pulsation, f being the frequency and $j^2 = -1$.
The storage modulus E' varies from 0.7 MPa at low frequency, to 2200 MPa at high frequency, corresponding to a ratio of 3000 between the glassy modulus and the rubbery modulus. This impressive fall of the storage modulus at the glass transition state is accompanied by the rise of the loss factor $\tan(\delta)$. Indeed the DMA results highlight very interesting tBA/PEGDMA viscoelastic properties: the value of the loss factor is higher than 1.5 in a wide range of frequencies and can reach a maximal value of 2.4.

2.3. SMP viscoelastic model

A viscoelastic model is chosen to describe the mechanical behavior of the tBA/PEGDMA on a wide band of frequency and temperature [31]. The 2S2P1D model, whose name comes from the abbreviation of the combination of two Springs, two Parabolic creep element and one Dashpot [33, 34], is used for the description of the rheological properties of the viscoelastic material. The complex modulus E^* is estimated by

$$E^*(\omega, T) = E_0 + \frac{E_\infty - E_0}{1 + \gamma(j\omega\tau)^{-k} + (j\omega\tau)^{-h} + (j\omega\beta\tau)^{-1}} \ , \tag{3}$$

where k and h are exponents with $0 < k < h < 1$, γ and β are constants, E_0 is the rubber modulus when $\omega \to 0$, E_∞ is the glassy modulus when

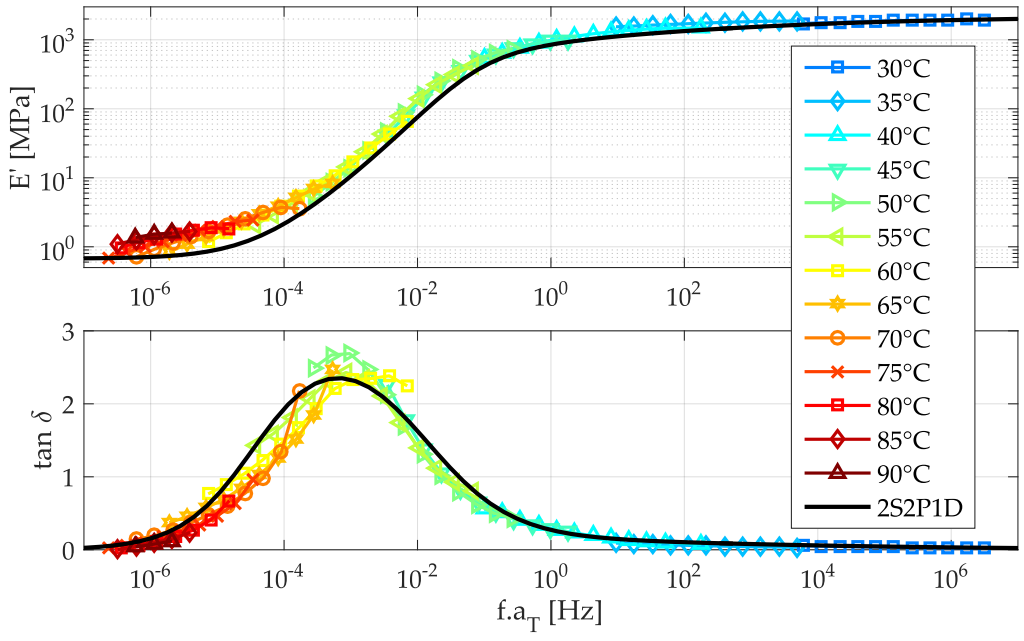

Figure 1: Master curves of the storage modulus E' and the loss factor tan(δ) according to the reduced frequency $f.a_T$ at a reference temperature $T_0 = 40°C$ and the comparison with the viscoelastic model 2S2P1D (black continuous line).

$\omega \to \infty$. τ is the characteristic time, estimated by the Time-Temperature Superposition Principle:

$$\tau(T) = a_T(T).\tau_0 \ , \tag{4}$$

where $a_T(T)$ is the shift factor at the temperature T and $\tau_0 = \tau(T_0)$ is determined at the reference temperature T_0.

The mechanical representation of the model is shown in Figure 2(a), together with the corresponding strain-stress loop of the material for permanent harmonic motion in time domain (Figure 2(b)). The 2S2P1D model parameters for the tBA/PEGDMA, determined through least-square curve fitting technique, are given in Table 1.

Table 1: 2S2P1D model parameters for the tBA/PEGDMA.

E_0 (MPa)	E_∞ (MPa)	k	h	γ	β	τ_0 (s)
0.67	2211	0.16	0.79	1.68	3.8e+4	0.61

As it can be seen in Figure 1, a good fit is obtained between the 2S2P1D model and the experimental measurements, over a wide frequency band. Thus, the 2S2P1D model will be used to discuss the damping properties of the SMP (Section 3) and to describe the tBA/PEGDMA mechanical properties in the Finite Element model used in Section 4.

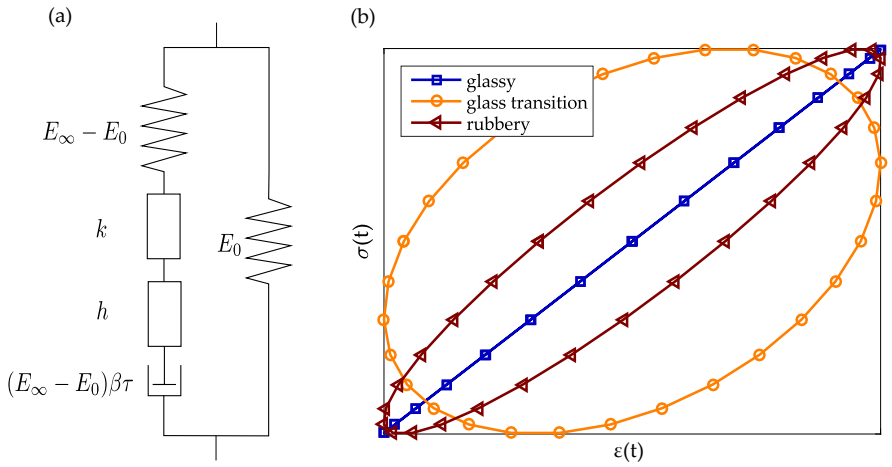

Figure 2: (a) Mechanical representation of the 2S2P1D model. k and h are two parabolic creep elements. (b) Strain-stress loop of the material in time domain.

3. Damping control

The expression of the complex modulus E^* (Eq. 3) obtained through the 2S2P1D model provides the mechanical properties in the temperature and frequency ranges of interest. It is then possible, for a frequency set, to determine the optimum temperature to get a maximum damping corresponding to the loss factor peak. For example, as shown in Figure 3, if the target frequency is 200 Hz, the temperature corresponding to maximal damping is 72°C where the loss factor reaches its maximum value. The same kind of curve can be plot for multiple frequencies. An objective damping ratio at a given frequency can then be obtained using this approach.

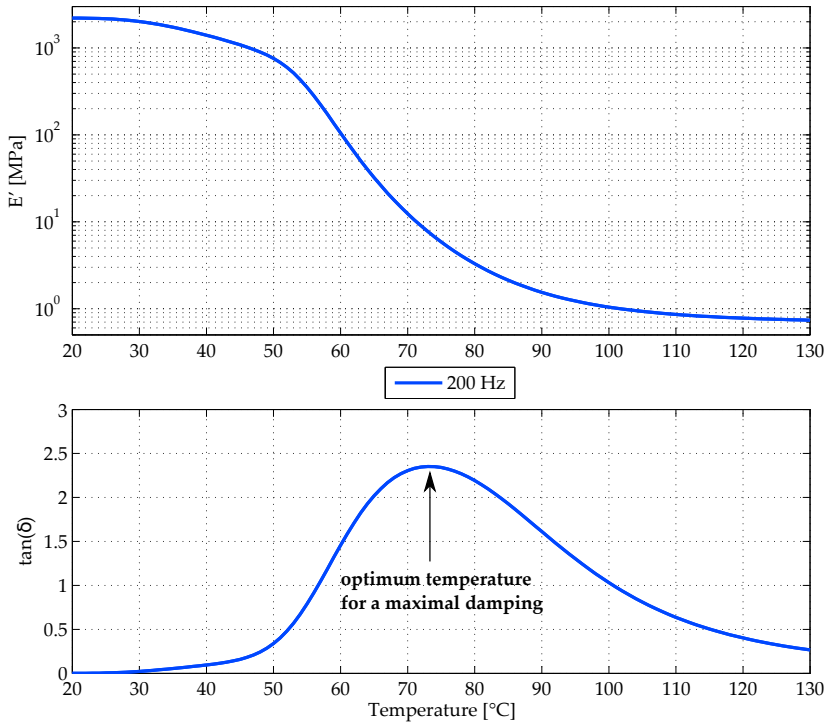

Figure 3: Storage modulus E' and loss factor tan(δ) obtained using the 2S2P1D model at 200 Hz to determine the temperature for a maximum damping (72°C in this case).

However in most practical cases, the designer will be interested in obtaining highest damping values in a wide frequency band. This case is considered in the following. The Figure 4 shows the mechanical properties for 20 frequencies between 100 and $10,000$ Hz. This rainbow calibration curve allows to determine the optimum temperature for maximum damping at different frequencies: at 100 Hz the optimal temperature is 71°C, at 885 Hz it is 82°C, at $2,975$ Hz it is 90°C or at $10,000$ Hz it is 104°C. For one frequency set, one temperature allows to damp efficiently the structure. But for many practical applications, one can be interested to damp a SMP complex structure on a large frequency band for example between 100 Hz and $10,000$ Hz. The optimum temperature is therefore not anymore the temperature of the peak of the loss factor but the intersection of the loss factor curves. In this case the rainbow calibration curve (Figure 4) can be used: the mechanical properties are plotted on the frequency range of interest and for several temperatures, the intersection of the loss factor curves is the optimum temperature. Indeed, this intersection is the best compromise to damp the structure on the entire frequency band set, in the considered case the loss factor value is over 1.7 for each frequency in the band of interest.

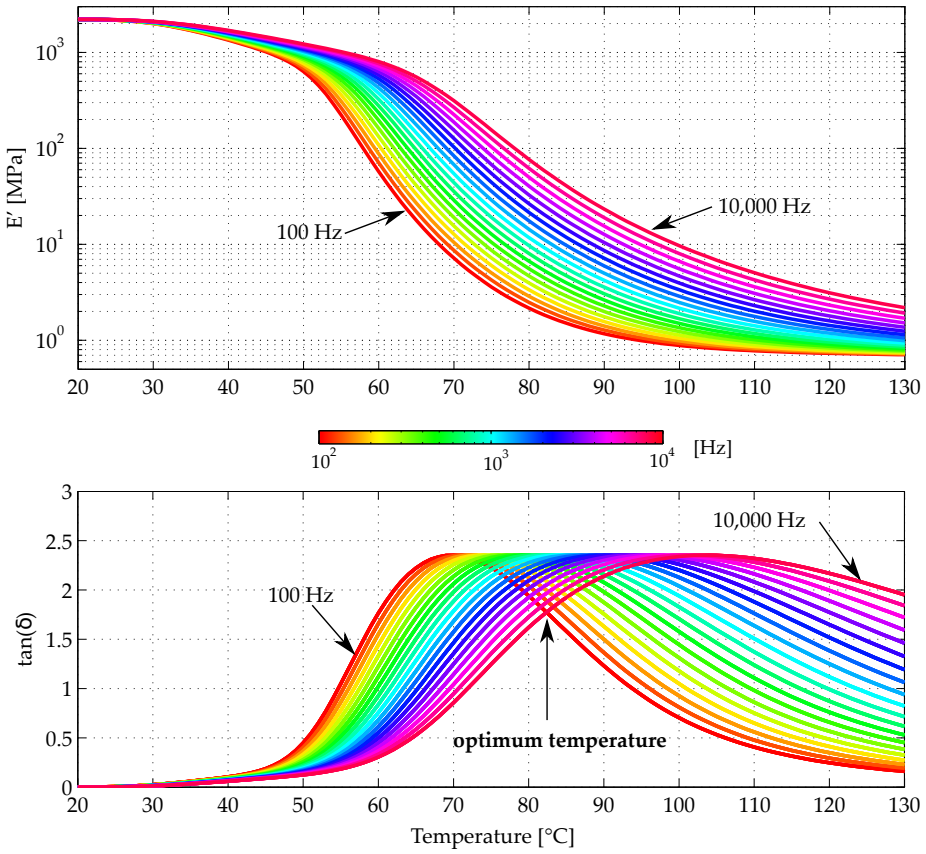

Figure 4: Rainbow calibration curve : storage modulus E' and loss factor tan(δ) obtained using the 2S2P1D model in the [100 - 10,000] Hz frequency range to obtain the optimum damping temperature, at the loss factor curves intersection (81°C in this case).

Furthermore, the Figure 5 illustrates the extent of possibilities of the tBA/PEGDMA when used as vibration control device. This figure provides the temperature ranges corresponding to target loss factors of 1, 1.5, 2 or the maximum value 2.4 in given frequency ranges. Thereby for a temperature tune between 30°C and 100°C the tBA/PEGDMA can damp very low frequencies (10^{-5} Hz) to high frequencies (10^{5} Hz). Thus the proper tune

of the Shape Memory Polyper temperature permits to damp vibrations on a large scale of frequencies.

In the next section, this tunable damping concept is investigated through the integration of the tBA/PEGDMA SMP in a composite structure.

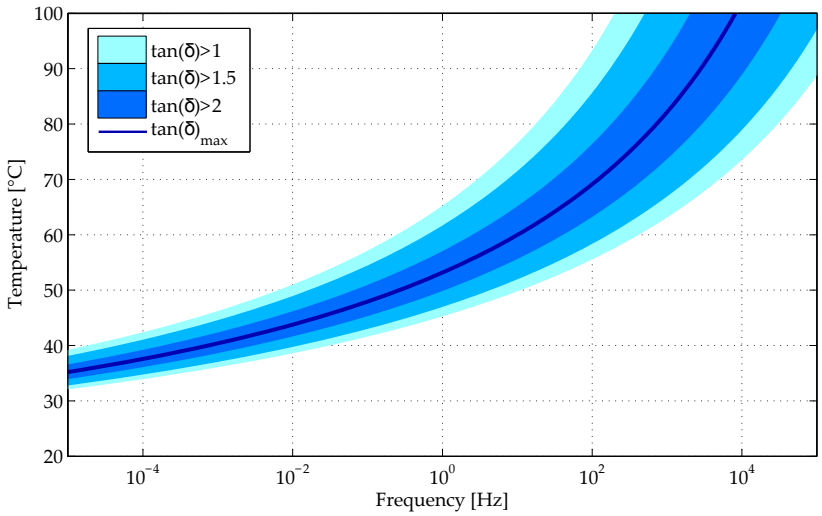

Figure 5: Values of temperature and frequency to have $\tan(\delta)>1$, $\tan(\delta)>1.5$, $\tan(\delta)>2$ or $\tan(\delta)=2.4$ maximum, obtained using the 2S2P1D model.

4. Design of a SMP composite structure

The structure of interest is a composite sandwich structure (Figure 6). Its dimensions are 120 mm $\times$ 50 mm and 3.2 mm thick. The SMP core is 2.2 mm thick, and the aluminum skins are 0.5 mm thick.

A Finite Element model of this composite sandwich is built on Comsol Multiphysics 4.4. The sandwich composite is meshed with solid quadratic Lagrange elements with one element in the thickness of the aluminum skins

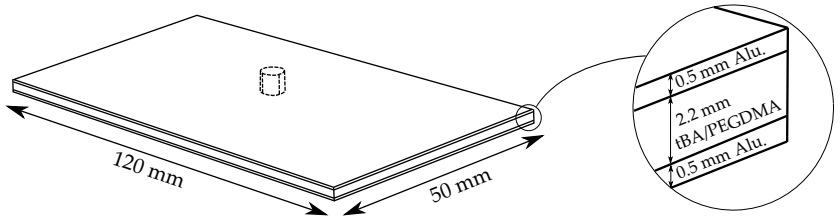

Figure 6: Sandwich structure used in numerical simulation and in experimental tests (magnet in dotted line, used for the experimental excitation).

and two elements in the SMP core thickness. The Finite Element model has 51,928 elements and 172,300 degrees of freedom. The convergence of the mesh on the frequency band of interest has been checked.

The materials are assumed to be homogeneous and isotropic. The aluminum material properties for the skins are given in Table. 2. The SMP core material properties are taken from Butaud et al. [31]: 0.37 for the Poisson's ratio ν (determined from quasi-static tests) and 990 kg/m^3 for the mass density (determined with a pycnometer). The complex modulus for the SMP core is given in Equation (3).

A harmonic point force is located on the upper skin at 7 mm from the center of the sandiwch. Free boundary conditions are used in the simulations.

Table 2: Aluminum material properties for the skins in the Finite Element model.

E (GPa)	ν	ρ (kg/m^3)	η
70	0.33	2700	0.01

The Frequency Response Function (FRF) of the sandwich structure is obtained through a direct Frequency Domain study, in the [100 - 10, 000] Hz

frequency range, from the Finite Element model. The mean square velocity FRF is calculated at several temperatures, between 20°C and 130°C every 10°C. The results of the simulations highlight the controllable character of the structural damping through the temperature. The impressive damping capacities of the SMP, which are temperature dependent, are shown in Figure 7. The results of four representative temperatures, at 20°C, 50°C, 80°C and 130°C, are presented.

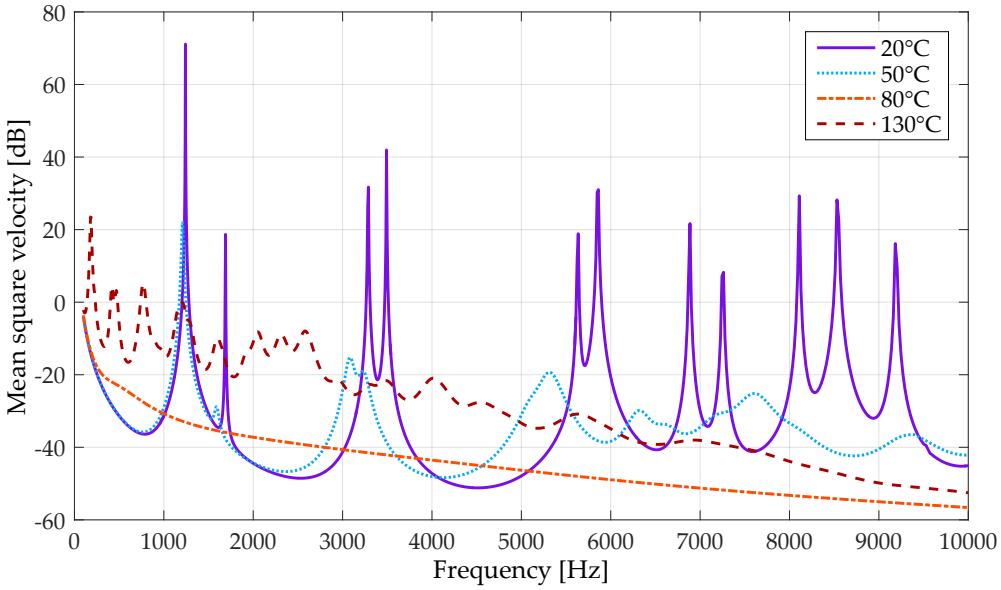

Figure 7: Simulation results at 20°C, 50°C, 80°C and 130°C.

At 20°C, the SMP is in the glassy state over the entire frequency range, with a high storage modulus around 2000 MPa, while the loss factor is very low, of the same order of magnitude as the one of the aluminum skins. The sandwich structure is then rigid but not damped and the FRF exhibits res-

onance peaks.

At 50°C, the SMP is close to the glass transition. The storage modulus is around 1000 MPa, and the loss factor has an average value of 0.2 over the frequency range. As seen in Figure 7, the structure heated at 50°C is comparable to a classical sandwich composite exhibiting damping effect through viscoelastic behavior of the core.

At 80°C, which is the optimum damping temperature (determined in Section 3), the tBA/PEGDMA is in the transition state where the material changes from glassy state to rubbery state. Compared to the configuration at 20°C, the SMP storage modulus is lower while the loss factor has increased, leading to the radical suppression of the sandwich structure resonances. Almost no dynamic effects are visible in the whole frequency range in the FRF amplitude: the curve is completely smoothed and the maximum velocity level is reduced of about 104 dB.

In the rubbery state, at 130°C, the storage modulus has a low value. The loss factor varies with frequency from 0.2 (at 100 Hz) to 2 (at 10 kHz), hence the sandwich FRF is not as damped as at 80°C, and some resonances are visible at low frequencies.

Thus, the Figure 7 shows the impressive damping properties of the tBA/-PEGDMA which are furthermore controllable by tuning the temperature of the sandwich core using the rainbow calibration curve (Figure 4(b)).

5. Validation and discussion

5.1. Experimental setup description and validation

The elaborated Shape Memory Polymer plate, 2.2 mm thick (± 0.1 mm due to the elaboration process), and the aluminum plates, 0.5 mm thick, are glued thanks to an epoxy structural adhesive Scotch-Weld^{TM} DP490 3M under pressure of 100 kPa during 24 hours. The composite sandwich is 3.2 mm (± 0.15 mm) thick.

The sandwich is placed on an elastic structure in order to assess free-free conditions. Contactless actuators and sensors are used. The external force is applied using a voice-coil actuator with a permanent magnet glued on the sandwich skin (Figure 8(a)). A broadband random excitation is applied between 100 and $10,000$ Hz. The plate response is measured with a laser vibrometer (Polytec OFV-505) focused on a reflecting sticker spread on the excitation point (Figure 8(b)). The Frequency Response Function (FRF) of the composite sandwich is then measured with a multi-channel spectral analyser. This assembly is placed in a thermal chamber (Climats EXCAL) with a temperature control between 20 and 130°C every 10°C (± 1°C).

Furthermore, in order to validate the repeatability of the experimental results, the measurements are done three times at each temperature. In order to check the stability of the SMP in temperature, the sandwich is heated and cooled: three temperature rises are performed with measurements every 10°C.

The experimental results measured several times at ambient temperature (20°C) are similar at each measurements, before or after the temperature rises. Thus, the gluing of the sandwich is efficient and the experimental

setup and procedures are very stable. Moreover a temperature rise at 130°C did not affect the mechanical properties of the structure, then there is no secondary polymerization of the SMP with the temperature rise. The stability of the tBA/PEGDMA is validated and thereby the stability of its mechanical properties and damping capacities.

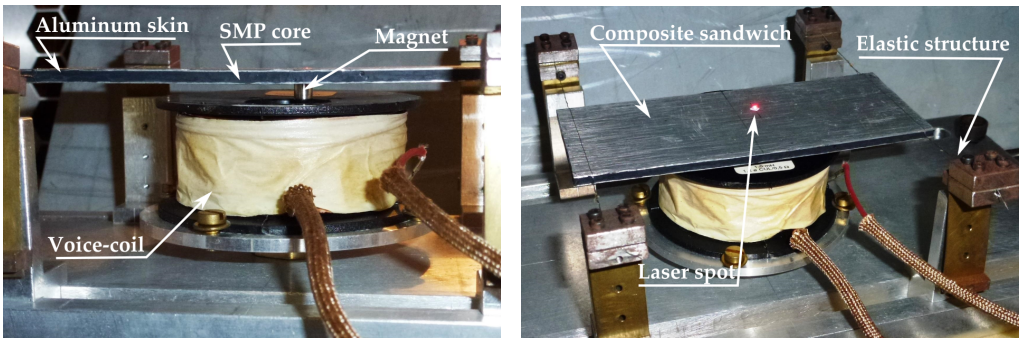

(a) Voice-coil actuator. (b) Laser vibrometer measurement.

Figure 8: Experimental setup

5.2. Model/test correlations

In this section, numerical results are compared to experimental tests. In Figure 9, the velocity collocated FRFs, measured at 20°C, 50°C, 80°C and 130°C, are compared to those obtained from the Finite Element model.

In Figure 9(a), the correlations at 20°C can be observed. The main trends of the dynamics are estimated by the model, even if some discrepancies appear. In the very low frequency range and at anti-resonances, the main differences are mostly due to the boundary conditions. Indeed, in the experimental setup, thin steel wires are used to support the sample (see Figure 8(b)), while free-free conditions are used in the model. A focus on the

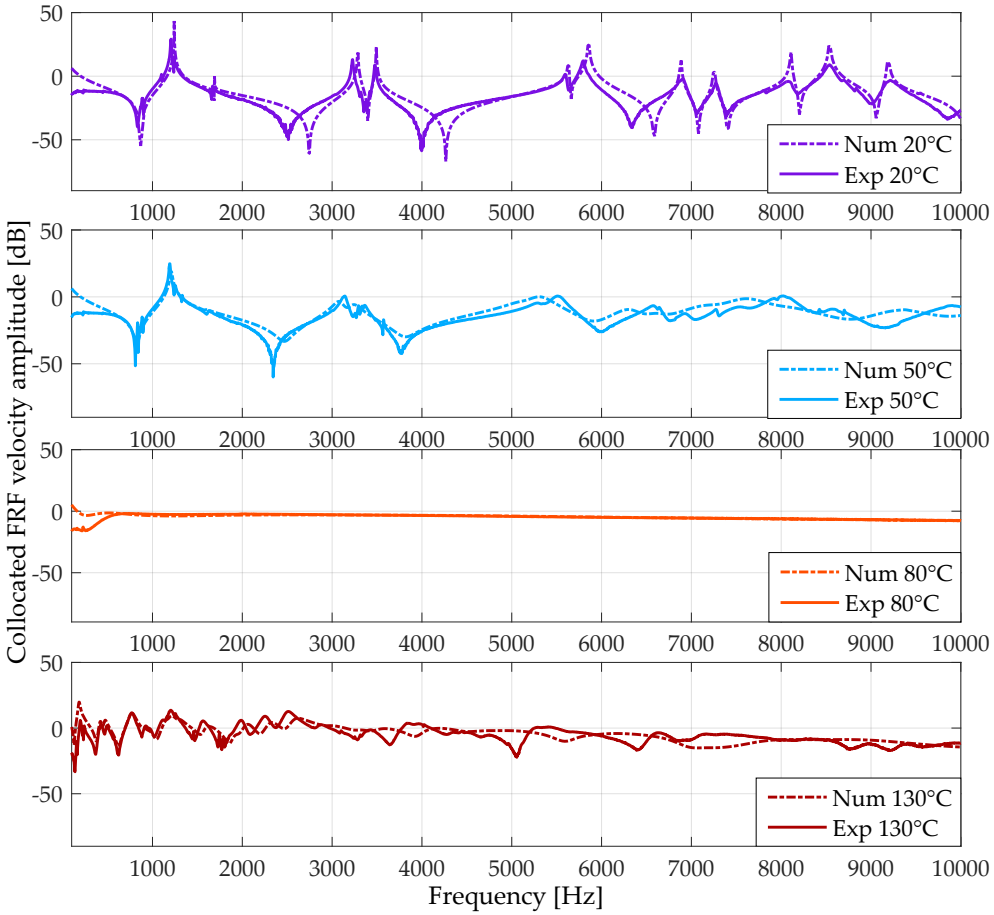

Figure 9: Experimental results "Exp" and simulation results "Num" at 20°C, 50°C, 80°C and 130°C.

resonances shows that the relative distance between numerical and experimental eigenfrequencies is less than 1% at 20°C. The Finite Element model is hence representative of the dynamic properties of the composite sandwich. The amplitude at resonances is not always properly estimated by the model. These errors on the damping properties can be explained by the large uncertainties on the aluminum and SMP loss factor values implemented in the

Finite Element model at 20°C. Indeed at ambient temperature the SMP loss factor is really low, and close to the aluminum loss factor value, which is found to be between 10^{-2} and 10^{-4} in literature [35, 36, 37]. Moreover, the asymptotic behavior of the 2S2P1D model yields an underestimation of the loss factor at this temperature. Hence, the damping loss factors of both materials have the same order of magnitude: the modal damping ratio is therefore unfortunately controlled by the aluminum loss factor. Efforts regarding the characterization of the loss factor for low values are still needed to improve the quality of the model.

A good correlation between the model and the experiments at 50°C can be observed in Figure 9(b). The relative distance between numerical and experimental eigenfrequencies is less than 3% at 50°C and the damping properties is better estimated because the SMP loss factor is higher, hence the global damping is less affected by the aluminum's loss factor.

Figure 9(c) illustrates once again the impressive damping capabilities of the SMP, which smooths all resonances. At this temperature, the correlation between the model and the experiments is excellent. As explained above, the difference in the very low frequency range is due to the boundary conditions.

Figure 9(d) shows that the model correlates quite well with the experiments at 130°C, despite of the quite complex mode shapes which are due to the very low stiffness of the core. Comments and conclusions are identical to those given at 50°C.

Finally, despite the various uncertainties (boundary conditions, thickness of the sandwich, gluing of the skins, ...), the correlation between the Finite Element model and the experimental results is really good. The model can then

be used for designing structures with high damping capabilities.

5.3. Discussion - extending the concept toward low frequencies

Due to the small size of the structure used in this work, the effectiveness of the approach has been demonstrated on the [1000-10,000] frequency range. The objective of this section is to show that the methodology is also applicable at lower frequencies. The Finite Element model, which has been validated in the previous section, is used for the analysis of a sandwich structure, a little larger (150×300 mm^2) than the one considered previously, and with the same thickness dimensions, fixed on the short edge and excited on one point on a corner. The simulation gives the five first eigenfrequencies between 33 Hz and 570 Hz. Thanks to the calibration curve, the optimal temperature is determined around 73°C for this frequency range of interest. The Frequency Response Function (FRF) of the sandwich structure is obtained through a direct Frequency Domain study, in the [1 - 620] Hz frequency range, from the Finite Element model. The mean square displacement FRF is calculated at 20°C and 73°C. The results of the simulations still highlight the impressive damping capacities of the SMP (Figure 10). We can notice that the dynamic damping is still very interesting at low frequency, even if the quasi-static behavior is affected (at 1 Hz the displacement amplitude is more important than at 73°C). It appears that a drawback of a good damping is then the loss of static rigidity. However for the five first eigenfrequencies, the rainbow calibration proves its efficiency again with a significant damping on the large frequency band of interest.

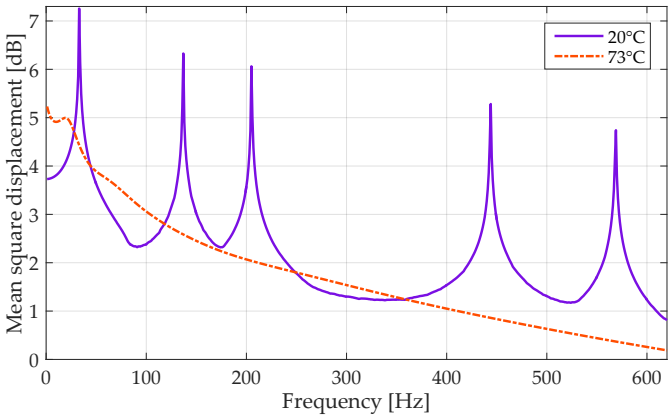

Figure 10: Simulation results at 20°C and 73°C between 1 Hz and 620 Hz.

6. Conclusion

This study highlights the awesome damping capacities of a Shape Memory Polymer through its use in a complex structures such as sandwich composites. These capacities are checked not only in Finite Element modeling but also experimentally. The tuning of the damping of the structure is performed thanks to the rainbow calibration curve. The ability of the Finite Element model through a viscoelastic law to represent the behavior of the sandwich is verified. A wide frequency and temperature range has been explored in experiment and simulation, the results demonstrate the impressive damping properties of the composite sandwich. The methodology which is proposed in this paper is applicable to any viscoelastic material exhibiting frequency - and temperature - dependent high damping properties.

Acknowledgment

The authors thank ACOEM/01dB-Metravib for the dynamic mechanical analysis of the tBA/PEGDMA.
This work was co-financed by The French National Research Agency under grant number ANR-12-JS09-008-COVIA. It has been performed in cooperation with the Labex ACTION program (ANR-11-LABX-0001-01).

[1] M. Behl, A. Lendlein, Shape-memory polymers, Materials today 10 (4) (2007) 20–28.

[2] B. Dietsch, T. Tong, A review-: Features and benefits of shape memory polymers (smps), Journal of advanced materials 39 (2) (2007) 3–12.

[3] Y. Liu, H. Du, L. Liu, J. Leng, Shape memory polymers and their composites in aerospace applications: a review, Smart Materials and Structures 23 (2) (2014) 023001.

[4] L. Sun, W. M. Huang, Z. Ding, Y. Zhao, C. C. Wang, H. Purnawali, C. Tang, Stimulus-responsive shape memory materials: a review, Materials & Design 33 (2012) 577–640.

[5] D. Ratna, J. Karger-Kocsis, Recent advances in shape memory polymers and composites: a review, Journal of Materials Science 43 (1) (2008) 254–269. doi:10.1007/s10853-007-2176-7.

[6] A. Lendlein, S. Kelch, Shape-memory polymers, Angewandte Chemie International Edition 41 (12) (2002) 2034–2057.

[7] Y. Tsai, C.-h. Tai, S.-J. Tsai, F.-J. Tsai, Shape memory effects of poly (ethylene terephthalate-co-ethylene succinate) random copolymers, European Polymer Journal 44 (2) (2008) 550–554.

[8] M. J. Barwood, C. Breen, F. Clegg, C. L. Hammond, The effect of organoclay addition on the properties of an acrylate based, thermally activated shape memory polymer, Applied Clay Science 102 (2014) 41–50.

[9] R. Biju, C. R. Nair, Synthesis and characterization of shape memory epoxy-anhydride system, Journal of Polymer Research 20 (2) (2013) 1–11.

[10] A. M. Ortega, S. E. Kasprzak, C. M. Yakacki, J. Diani, A. R. Greenberg, K. Gall, Structure–property relationships in photopolymerizable polymer networks: Effect of composition on the crosslinked structure and resulting thermomechanical properties of a (meth) acrylate-based system, Journal of applied polymer science 110 (3) (2008) 1559–1572.

[11] G. Tandon, K. Goecke, K. Cable, J. Baur, Durability assessment of styrene-and epoxy-based shape-memory polymer resins, Journal of Intelligent Material Systems and Structures 20 (17) (2009) 2127–2143.

[12] T. Xie, I. A. Rousseau, Facile tailoring of thermal transition temperatures of epoxy shape memory polymers, Polymer 50 (8) (2009) 1852–1856.

[13] G. Ellson, M. Di Prima, T. Ware, X. Tang, W. Voit, Tunable thiol–

epoxy shape memory polymer foams, Smart Materials and Structures 24 (5) (2015) 055001.

[14] P. Butaud, V. Placet, J. Klesa, M. Ouisse, E. Foltête, X. Gabrion, Investigations on the frequency and temperature effects on mechanical properties of a shape memory polymer (veriflex), Mechanics of Materials 87 (2015) 50–60.

[15] M. Sunar, S. Rao, Recent advances in sensing and control of flexible structures via piezoelectric materials technology, Applied Mechanics Reviews 52 (1) (1999) 1–16.

[16] M. Trindade, A. Benjeddou, R. Ohayon, Piezoelectric active vibration control of damped sandwich beams, Journal of Sound and Vibration 246 (4) (2001) 653–677.

[17] M. Collet, M. Ouisse, F. Tateo, Adaptive metacomposites for vibroacoustic control applications, Sensors Journal, IEEE 14 (7) (2014) 2145–2152.

[18] F. Tateo, M. Collet, M. Ouisse, K. Cunefare, Design variables for optimizing adaptive metacomposite made of shunted piezoelectric patches distribution, Journal of Vibration and Control (2014) 1077546314545100.

[19] M. D. Rao, Recent applications of viscoelastic damping for noise control in automobiles and commercial airplanes, Journal of Sound and Vibration 262 (3) (2003) 457–474.

[20] M. A. Trindade, Experimental analysis of active-passive vibration control using viscoelastic materials and extension and shear piezoelectric actuators, Journal of Vibration and Control (2010) 1077546309356042.

[21] P. Grootenhuis, The control of vibrations with viscoelastic materials, Journal of Sound and Vibration 11 (4) (1970) 421–433.

[22] A. Arajo, C. M. Soares, C. M. Soares, J. Herskovits, Optimal design and parameter estimation of frequency dependent viscoelastic laminated sandwich composite plates, Composite Structures 92 (9) (2010) 2321 – 2327, fifteenth International Conference on Composite Structures.

[23] P. Aumjaud, C. Smith, K. Evans, A novel viscoelastic damping treatment for honeycomb sandwich structures, Composite Structures 119 (2015) 322 – 332.

[24] J. Lifshitz, M. Leibowitz, Optimal sandwich beam design for maximum viscoelastic damping, International Journal of Solids and Structures 23 (7) (1987) 1027–1034.

[25] J. Li, Y. Narita, The effect of aspect ratios and edge conditions on the optimal damping design of thin soft core sandwich plates and beams, Journal of Vibration and Control (2012) 1077546312463756.

[26] J.-M. Berthelot, M. Assarar, Y. Sefrani, A. E. Mahi, Damping analysis of composite materials and structures, Composite Structures 85 (3) (2008) 189 – 204.

[27] N. Okubo, Preparation of master curves by dynamic viscoelastic measurements, SII NanoTechnology Inc. 6 (1990).

[28] B. C. Chun, S. H. Cha, Y.-C. Chung, J. W. Cho, Enhanced dynamic mechanical and shape-memory properties of a poly (ethylene terephthalate)–poly (ethylene glycol) copolymer crosslinked by maleic anhydride, Journal of applied polymer science 83 (1) (2002) 27–37.

[29] V. Srivastava, S. a. Chester, L. Anand, Thermally actuated shape-memory polymers: Experiments, theory, and numerical simulations, Journal of the Mechanics and Physics of Solids 58 (8) (2010) 1100–1124.

[30] C. M. Yakacki, R. Shandas, C. Lanning, B. Rech, A. Eckstein, K. Gall, Unconstrained recovery characterization of shape-memory polymer networks for cardiovascular applications, Biomaterials 28 (14) (2007) 2255 – 2263.

[31] P. Butaud, M. Ouisse, V. Placet, E. Foltête, Experimental investigations on viscoelastic properties of a shape memory polymer, in: ASME 2014 Conference on Smart Materials, Adaptive Structures and Intelligent Systems, American Society of Mechanical Engineers, 2014, pp. V001T01A029–V001T01A029.

[32] M. L. Williams, R. F. Landel, J. D. Ferry, The temperature dependence of relaxation mechanisms in amorphous polymers and other glass-forming liquids, Journal of the American Chemical Society 77 (14) (1955) 3701–3707.

[33] N. I. M. Yusoff, D. Mounier, G. Marc-Stphane, M. R. Hainin, G. D. Airey, H. D. Benedetto, Modelling the rheological properties of bitumi-

nous binders using the 2s2p1d model, Construction and Building Materials 38 (0) (2013) 395 – 406.

[34] E. Gourdon, C. Sauzéat, H. Di Benedetto, K. Bilodeau, Seven-parameter linear viscoelastic model applied to acoustical damping materials, Journal of Vibration and Acoustics 137 (6) (2015) 061003.

[35] K. Ege, T. Boncompagne, B. Laulagnet, J.-L. Guyader, Experimental estimations of viscoelastic properties of multilayer damped plates in broad-band frequency range, arXiv preprint arXiv:1210.3333 (2012).

[36] M. Thomas, F. Laville, Simulation des vibrations mécaniques, Presses de l'Université du Québec, 2007.

[37] F. Orban, Damping of materials and members in structures, in: Journal of Physics: Conference Series, Vol. 268, IOP Publishing, 2011, p. 012022.